

# Efficiency improvement of a DC/DC converter using LTCC substrate

Dong Yun Jung  | Hyun Gyu Jang  | Minki Kim | Junbo Park  |  
Chi-Hoon Jun | Jong Moon Park | Sang Choon Ko

ICT Materials & Components  
Research Laboratory, Electronics and  
Telecommunications Research Institute,  
Deajeon, Rep. of Korea

## Correspondence

Dong Yun Jung, ICT Materials &  
Components Research Laboratory,  
Electronics and Telecommunications  
Research Institute, Deajeon, Rep. of Korea  
Email: dyjung14@etri.re.kr

## Funding information

This work was supported by the R&D  
program of MSIP/COMPA (No.  
2016K000251, Next Generation High  
Efficiency 3-Dimensional Convergence  
Power Conversion Module,) and IITP/MSIT  
(No. 2018-0-01138, Development of multi-  
layer ferrite power inductor and slim DC/  
DC converter).

We propose a substrate with high thermal conductivity, manufactured by the low-temperature co-fired ceramic (LTCC) multilayer circuit process technology, as a new DC/DC converter platform for power electronics applications. We compare the reliability and power conversion efficiency of a converter using the LTCC substrate with the one using a conventional printed circuit board (PCB) substrate, to demonstrate the superior characteristics of the LTCC substrates. The power conversion efficiencies of the LTCC- and PCB-based synchronous buck converters are 95.5% and 94.5%, respectively, while those of nonsynchronous buck converters are 92.5% and 91.3%, respectively, at an output power of 100 W. To verify the reliability of the LTCC-based converter, two types of tests were conducted. Storage temperature tests were conducted at  $-20^{\circ}\text{C}$  and  $85^{\circ}\text{C}$  for 100 h each. The variation in efficiency after the tests was less than 0.3%. A working temperature test was conducted for 60 min, and the temperature of the converter was saturated at  $58.2^{\circ}\text{C}$  without a decrease in efficiency. These results demonstrate the applicability of LTCC as a substrate for power conversion systems.

## KEYWORDS

DC/DC converter, efficiency, low-temperature co-fired ceramic, reliability test, thermal conductivity

## 1 | INTRODUCTION

There has been growing interest in the development of better technologies to improve the heat dissipation, thermal reliability, and efficiency of switching-mode power electronic products. Thermal issues have become critical in the design of power conversion systems. With increases in temperature, the on-resistance of a MOSFET ( $R_{ds,on}$ ), and the resistance and leakage current of a diode increase. High temperature also degrades the performance of passive devices such as inductors, capacitors, and resistors. Conventional systems using a printed circuit board (PCB) require additional cooling elements for heat dissipation, thereby increasing the overall size of the system.

The thermal conductivity of low-temperature co-fired ceramic (LTCC) is more than 10 times higher than that of an FR-4 PCB in power electronics applications. Notably, through-hole vias in a conventional PCB are electroplated with copper, while embedded vias used in LTCC are filled with silver. This enables an improvement in the power efficiency and optimizes the system volume. LTCC multilayer technology can further reduce the size of a system through three-dimensional high integration, embedding both active and passive devices. Table 1 compares the properties of a traditional PCB and the proposed LTCC substrate material.

Our group has studied discrete power device packages with an embedded cavity in multilayer LTCC to reduce the parasitic

**TABLE 1** Comparison of substrate material properties

		PCB	LTCC
Thermal Conductivity (W/mK)		0.2–0.4	4–5
Coefficient of thermal expansion (ppm/°C)		13–17	5–7
Heat dissipation		Low	High
Circuit	Layer	Cu foil	Ag paste
	Thermal Conductivity (W/mK)	385	419
	Electrical Resistivity ( $\mu\Omega\text{-cm}$ )	1.7	1.55
Substrate layer		FR-4	Ceramics
Cost		Low	Medium

inductance caused by wire bonding [1,2]. Virginia's Polytechnic Institute and State University has studied planar inductors using magnetic tape and a multilayer LTCC manufacturing process to implement small-size non-isolated point-of-load (POL) converters [3–6]. However, their maximum output power achieved is below 50 W, and the maximum output efficiency is 92.5% at an output power of approximately 6 W [3].

The 48-V system including a 48-to-12 V converter is applied in various fields, such as vehicles, servers, industrial power supplies, telecom, etc. In automotive applications, a 48-V system can achieve high efficiency and reduces wiring and component weight. Meanwhile, a 48-to-12 V converter is required for providing power to different types of electrical loads [7–9] for example, servers in data centers require 48-to-12 V converters with high efficiency and power density [10–12].

This paper discusses the applicability of a substrate with high thermal conductivity fabricated with LTCC process technology as a new DC/DC converter platform in power electronics applications. It also details the design of a 48-to-12 V converter, provides an efficiency comparison to four

other converters, and describes the results of a reliability test of the proposed LTCC-based nonsynchronous buck converter. The following four types of converters are designed and discussed in this paper:

1. (Type I) synchronous buck converter on LTCC
2. (Type II) synchronous buck converter on PCB
3. (Type III) nonsynchronous buck converter on LTCC
4. (Type IV) nonsynchronous buck converter on PCB

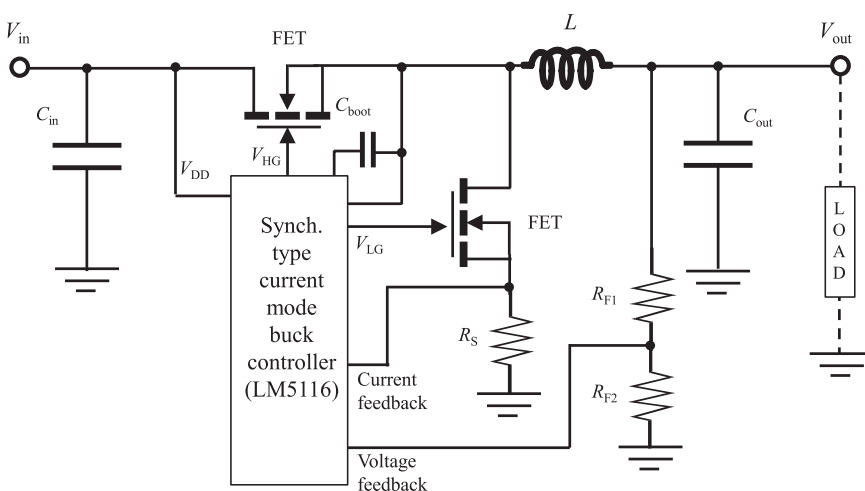
Section 2 of this paper discusses the design of a 48-to-12 V synchronous buck converter and compares the efficiencies of the proposed LTCC- and conventional PCB-based converters. Section 3 discusses the design of a 48-to-12 V nonsynchronous buck converter and compares the efficiencies of the proposed LTCC- and conventional PCB-based converters in a higher heat generation scenario. Finally, we report the reliability tests of the proposed LTCC-based converter.

## 2 | PROPOSED LTCC-BASED SYNCHRONOUS BUCK CONVERTER

We designed a synchronous converter and manufactured two converters, one using LTCC (Type I) and the other using a conventional PCB (Type II) for the substrates. Figure 1

**TABLE 2** Major design parameters of the synchronous buck converter

	Model/parameters
FET	GS61008P ( $R_{ds,on} = 10 \text{ m}\Omega$ )
$L$	10 $\mu\text{H}$ (27 $\text{m}\Omega$ )
$C_{out}$	594.11 $\mu\text{F}$
$C_{in}$	23.6 $\mu\text{F}$
Controller	LM5116

**FIGURE 1** Simplified circuit diagram of the 48-to-12 V synchronous buck converter

shows a simplified circuit diagram of the 48-to-12 V synchronous buck converter.

We used gallium nitride (GaN) FETs as the power switches. The fast switching speed, and low switching and conduction losses of a GaN-based power semiconductor enable small-size, highly efficient power conversion systems to be implemented [13–18]. Several research groups have reported highly efficient and small-size power conversion systems such as buck converters, boost converters, and inverters using GaN switching power devices [6,12,19–21]. In our design, an LM5116 was used as a pulse width modulation (PWM) controller to drive the high- and low-side power switches simultaneously.

Table 2 summarizes the major design parameters used in the synchronous buck converter, where  $L$ ,  $C_{in}$ , and  $C_{out}$  are selected using (1)–(3). Here,  $\Delta I$  is an inductor ripple current,  $f_{sw}$  is the switching frequency, and  $\Delta V$  is the maximum output voltage overshoot.

$$L = (V_{in,max} - V_{out}) \times \frac{V_{out}}{V_{in,max}} \times \frac{1}{f_{sw}} \times \frac{1}{\Delta I}, \quad (1)$$

$$C_{out} = \frac{L \times \left( I_{out,max} + \frac{\Delta I}{2} \right)^2}{(\Delta V + V_{out})^2 - V_{out}^2}, \quad (2)$$

$$C_{in} = I_{out,max} \times \frac{\sqrt{V_{out} \times (V_{in} - V_{out})}}{V_{in}}. \quad (3)$$

Figure 2 shows the breakdown of the power losses calculated by (4)–(8) in the synchronous buck converter. The expected efficiency of the 48-to-12 V synchronous buck converter is 95.44% at a maximum output power of 120 W.

$$P_{loss,C_{in}} = I_{ripple,in}^2 \times ESR_{C_{in}}, \quad (4)$$

$$P_{loss,H-FET} = \left[ I_{load}^2 \times R_{ds,on} \times \frac{V_{out}}{V_{in}} \right] + \left[ (V_{in} - V_{out}) \times \frac{I_{load}}{2} \times (t_r + t_f) \times f_{sw} \right] + \left[ C_{oss} \times (V_{in} - V_{out})^2 \times f_{sw} \right], \quad (5)$$

$$P_{loss,Inductor} = I_{load}^2 \times DCR_{Inductor}, \quad (6)$$

$$P_{loss,C_{out}} = I_{ripple,out}^2 \times ESR_{C_{out}}, \quad (7)$$

$$P_{loss,L-FET} = I_{load}^2 \times R_{ds,on} \times \left( 1 - \frac{V_{out}}{V_{in}} \right). \quad (8)$$

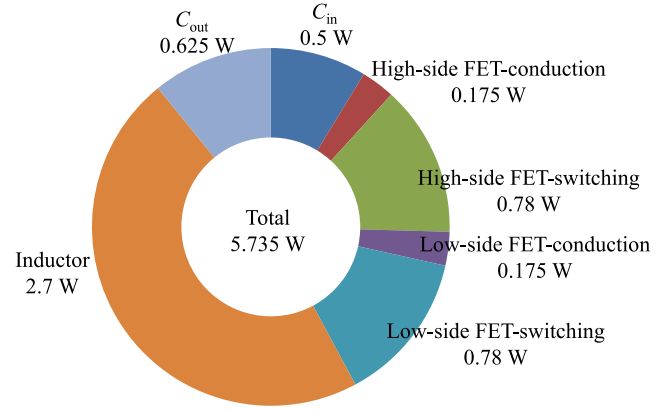


**FIGURE 2** Breakdown of the calculated power losses in the synchronous buck converter

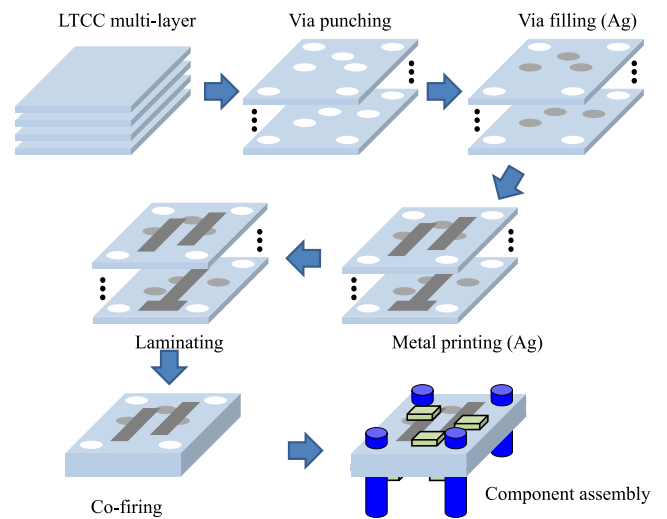


**FIGURE 3** Simplified manufacturing process of the proposed LTCC-based converter

Figure 3 shows the simplified manufacturing process of the proposed LTCC-based converter. Unlike the through-hole vias used in a conventional PCB process, which are electroplated with copper, vias used in the LTCC process are filled with silver. This reduces the parasitic inductance and improves the electrical and thermal conductivities. Because the standard thickness of LTCC tape is 100  $\mu\text{m}$ , and many layers are used in power electronics applications, a substantial amount of substrate noise reduction and high design flexibility of the control block, power, and ground planes can be achieved.

Figure 4 shows top and bottom views of the manufactured synchronous converter using an LTCC substrate. The size of the nonsynchronous converter is 55 mm  $\times$  40 mm and the thickness of the LTCC substrate is 1000  $\mu\text{m}$ .

To compare the performance of the LTCC and PCB, we manufactured two converters, one using LTCC (Type I) and the other using a conventional PCB (Type II), using the

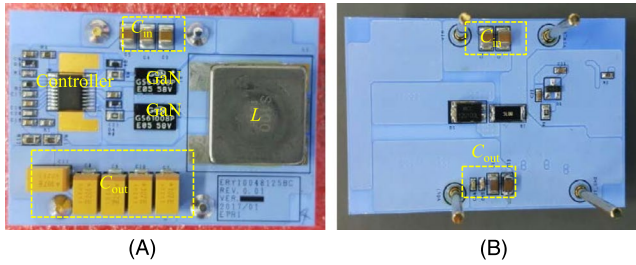


**FIGURE 4** (A) Top and (B) bottom views of the manufactured LTCC-based synchronous buck converter

circuit schematic of Figure 1. Figure 5 shows the waveforms of the gate voltage of the high-/low-side FETs, source voltage of the high-side FETs, and inductor current. Because the proposed Type I using the embedded metal planes and vias in the multilayer LTCC substrate has low parasitic inductance and capacitance, the noise and voltage spikes of the Type I are lower than those of the Type II.

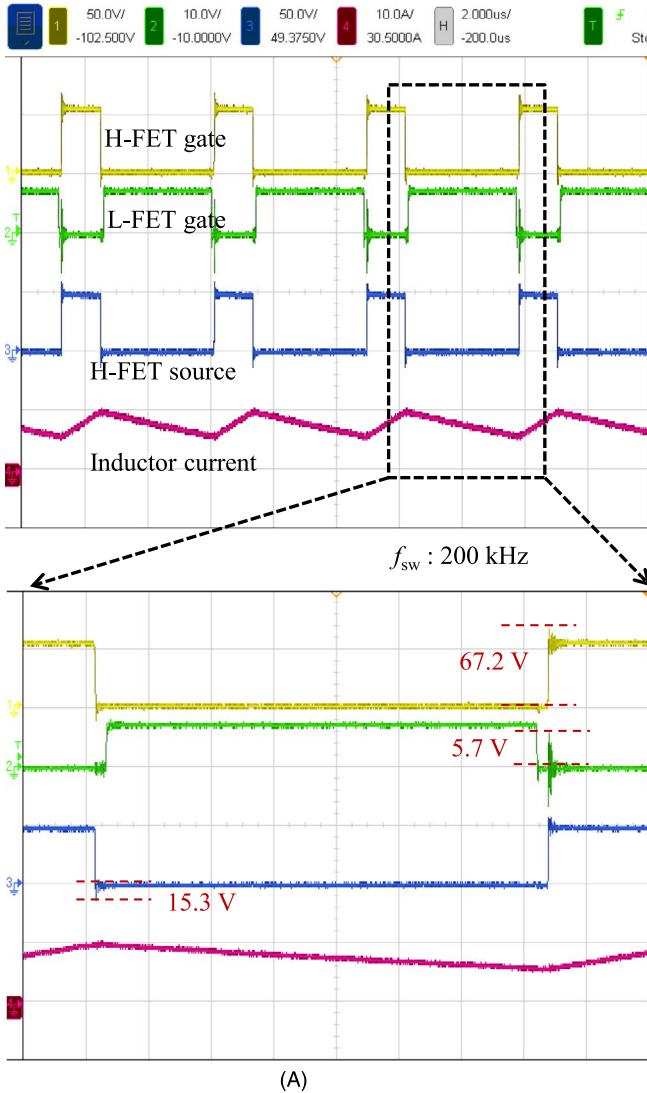
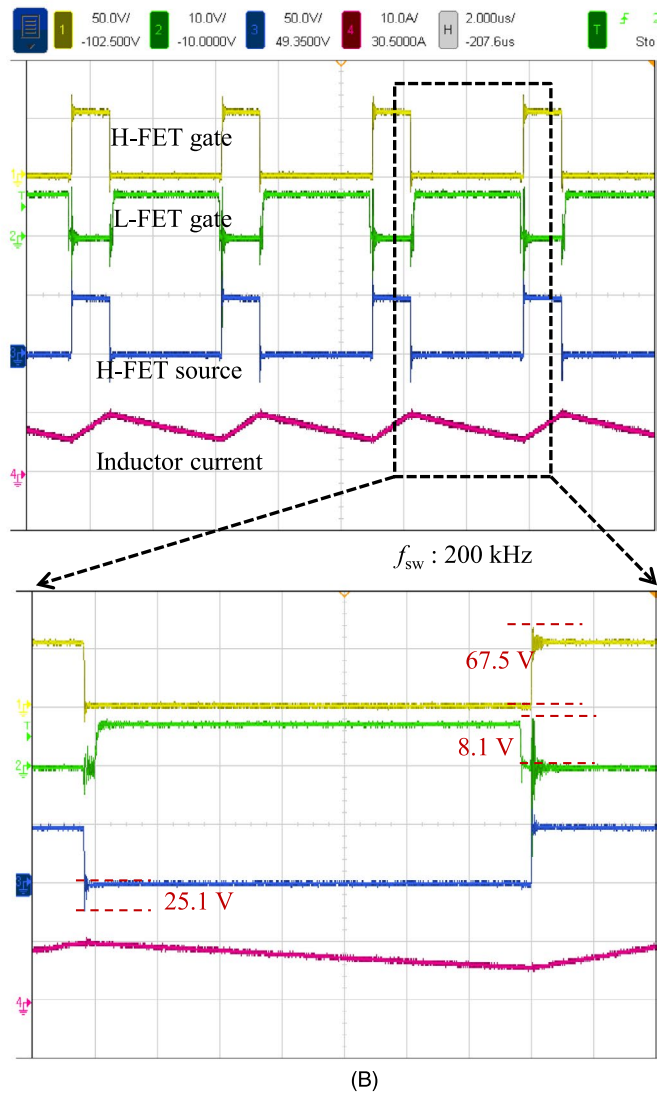


Figure 6 shows the measured power conversion efficiency at an input voltage of 48 V. The efficiencies of the LTCC- and PCB-based converters are 95.5% and 94.5%, respectively, at an output power of 100 W. As the output power increases, the difference in their efficiencies increases owing to the increased heat generation in the active elements.

### 3 | PROPOSED LTCC-BASED NONSYNCHRONOUS BUCK CONVERTER

To compare the efficiency under higher heat generation, we designed a 48-to-12 V nonsynchronous buck converter, as shown in Figure 7.

A GaN-based FET and Schottky barrier rectifier (SBR) are used as the power switch and freewheeling diode, respectively. We used an LM5088 as the PWM controller. The output of the LM5088 is fed to an LM5113 used as a gate driver. A low drop



**FIGURE 5** Measured voltage and current waveforms of the (A) Type I and (B) Type II systems

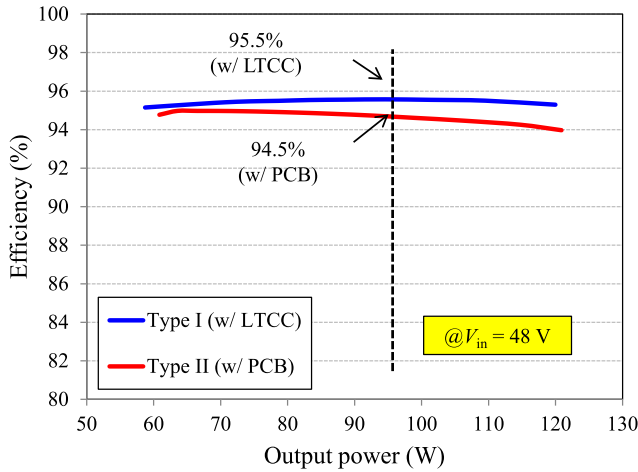


**FIGURE 6** Measured efficiency as a function of output power

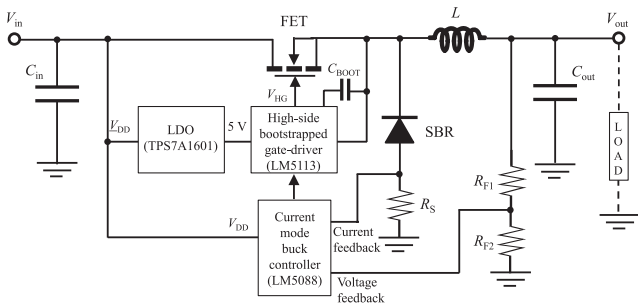


**FIGURE 7** Simplified circuit diagram of the 48-to-12 V nonsynchronous buck converter

out (LDO) regulator, TPS7A1601-Q1, is used to supply 5 V to the gate driver. During the on-state, the LM5113 provides 5 V at the gate of the FET. Table 3 summarizes the major design parameters used in the nonsynchronous buck converter.

Figure 8 shows the breakdown of the power losses calculated by (4)–(7) and (9) for the nonsynchronous converter. The expected efficiency of the designed 48-to-12 V nonsynchronous buck converter is 92.82% at a maximum output power of 120 W. Although the diode has a superior forward performance with a low  $V_f$  of 0.43 V and a forward current of 10 A at a forward voltage of 0.6 V, the diode power loss of 4.5 W makes up the largest portion of the total power loss of the converter. The inductor power loss is caused by a DC resistance (DCR) of 27 m $\Omega$ . This is directly proportional to the inductor size, and is therefore not discussed further.

$$P_{\text{loss,diode}} = \left(1 - \frac{V_{\text{out}}}{V_{\text{in}}}\right) \times I_{\text{load}} \times V_F. \quad (9)$$

Figure 9 shows top and bottom views of the manufactured nonsynchronous converter using LTCC. The size of the converter is 55 mm  $\times$  40 mm, and the thickness of the LTCC substrate is 1000  $\mu\text{m}$ .

**TABLE 3** Major design parameters of the nonsynchronous buck converter

Model/parameters	
FET	GS61008P ( $R_{\text{ds,on}} = 10 \text{ m}\Omega$ )
Diode	MBR12U100L ( $V_f = 0.43 \text{ V}$ )
$L$	10 $\mu\text{H}$ (DCR = 27 m $\Omega$ )
$C_{\text{out}}$	594.11 $\mu\text{F}$
$C_{\text{in}}$	23.6 $\mu\text{F}$
Controller	LM5088
Gate driver	LM5113
LDO	TPS7A1601-Q1

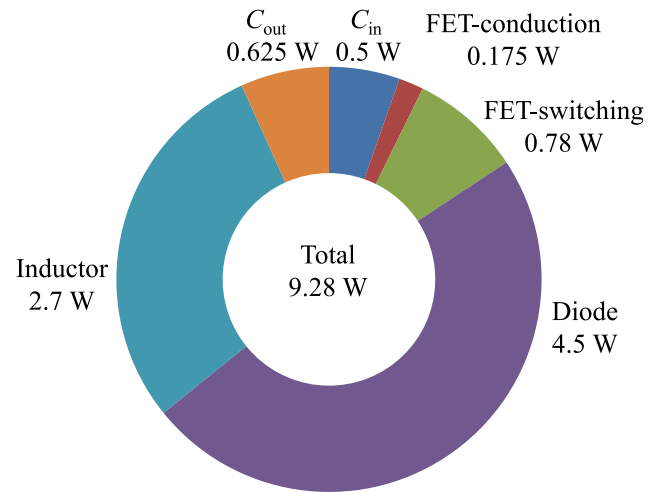


**FIGURE 8** Breakdown of the calculated power losses in the nonsynchronous buck converter

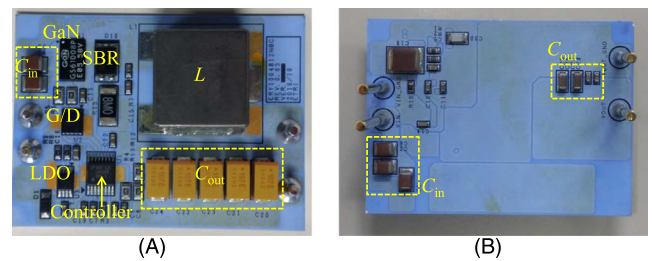


**FIGURE 9** (A) Top and (B) bottom views of the manufactured LTCC-based nonsynchronous buck converter

To compare the performances of the LTCC and PCB devices, we manufactured two converters, one using LTCC (Type III) and the other using a conventional PCB (Type IV), using the circuit design of Figure 7. Figure 10 shows the power conversion efficiency at an input voltage of 48 V. The efficiencies of the two converters are 92.5% and 91.3%, respectively, at an output power of 100 W. As



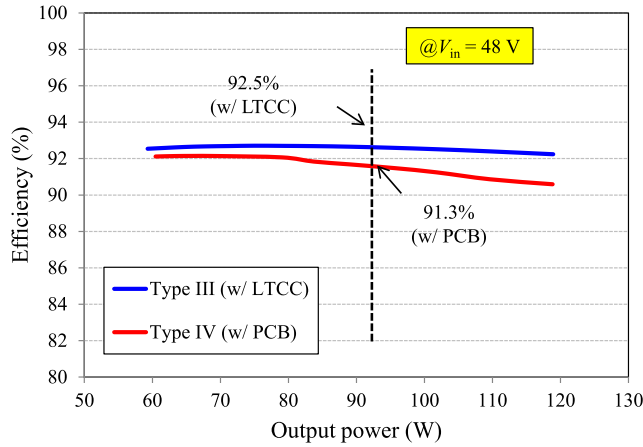


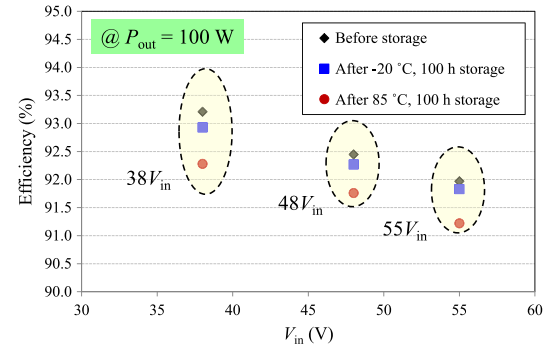
**FIGURE 10** Measured efficiency as a function of output power

with the synchronous buck converters, we can see that as the output power increases, the difference in their efficiencies increases owing to the increased heat dissipation.

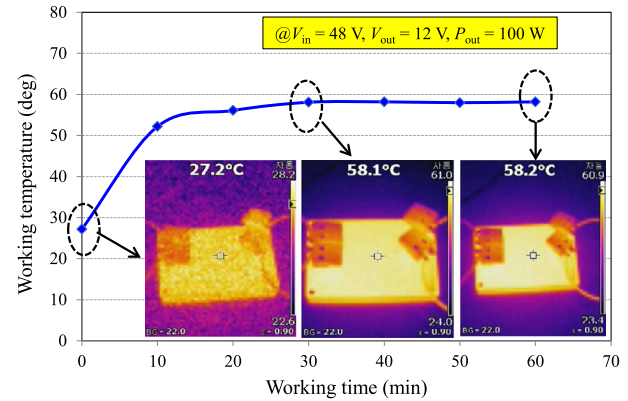
To verify the reliability of the LTCC based converter, two types of tests were conducted on the Type III converter: two storage temperature tests and a working temperature test. Storage temperature tests were conducted to compare the efficiency under normal operating conditions before and after storage in a chamber at  $-20^{\circ}\text{C}$  and  $85^{\circ}\text{C}$ , respectively, during a 100-h period. Figure 11 shows the variations in efficiency before and after the two storage tests. The observed variation in efficiency is less than 0.3%, demonstrating that the proposed converter achieves outstanding reliability.

Figure 12 shows the temperature variation of the converter as a function of the working time under an input voltage of 48 V, output voltage of 12 V, and output power of 100 W. The temperature variation was measured for 60 min, and the working temperature was increased from  $27.2^{\circ}\text{C}$  to  $58.2^{\circ}\text{C}$ . During the test, the efficiency of the converter remained constant, at approximately 92%.

Table 4 summarizes the performance comparison of previously reported LTCC-based converters with those presented in this work. Although the reported LTCC-based converters used a very high switching frequency of above



**FIGURE 11** Measured storage temperature test results of the proposed LTCC-based converter (Type III)



**FIGURE 12** Temperature variation of the LTCC-based converter (Type III) as a function of the working time at an input voltage of 48 V, output voltage of 12 V, and output power of 100 W

1 MHz to achieve a small form factor, their maximum output power is below 50 W, and their maximum output efficiency is 92.5% at an output power of approximately 6 W [3–6,12].

## 4 | CONCLUSION

We proposed a new platform using multilayer LTCC substrates for power electronics applications. Four types of buck

		$V_{in}$ (V)	$V_{out}$ (V)	Max. $P_{out}$ (W)	$f_{sw}$ (kHz)	Max. $\eta$ (@ $P_{out}$ ) (%) <sup>a</sup>
[3]		5	1.2	24	1300	92.5 (@6 W)
[4]		5	1.2	18	1500	89 (@8.4 W)
[5]		5	1.2	48	1500	89 (@24 W)
[6]		12	1.2	18	1000	91 (@9.6 W)
[12]		12	1.8	36	2000	88 (@19.8 W)
This Work	Type I	48	12	120	200	95.5 (@100 W)
	Type III	48	12	120	200	92.5 (@100 W)

**TABLE 4** Comparison of LTCC-based converters

<sup>a</sup>Expected maximum efficiency based on measured graphs.

converters, operating at 48-to-12 V, were manufactured using the proposed LTCC- and conventional PCB-based substrates to compare their efficiencies at high output power. The efficiencies of the LTCC- and PCB-based synchronous converters (Type I and Type II), and LTCC- and PCB-based nonsynchronous converters (Type III and Type IV) were 95.5% and 94.5%, and 92.5% and 91.3%, respectively, at an output power of 100 W. It was observed that as the output power increases, the difference in efficiency of the proposed LTCC- and conventional PCB-based converters increases owing to the increase in heat generation. Storage temperature and working temperature tests were carried out to evaluate thermal reliability. The LTCC substrate exhibited outstanding thermal reliability, which is approximately 10 times higher than that of a traditional PCB substrate. Based on a performance comparison between the proposed LTCC- and conventional PCB-based converters, we have demonstrated the potential of a multi-layer LTCC substrate for use in power electronics applications.

## ACKNOWLEDGMENTS

The authors thank Mr. Son with RN2 technologies (<http://rn2.co.kr>), and Mr. Lee with Y.tech (<http://www.ytcera.co.kr>), for their fabrication of the LTCC substrates.

## ORCID

Dong Yun Jung  <https://orcid.org/0000-0002-4793-7584>

Hyun Gyu Jang  <https://orcid.org/0000-0003-3502-1613>

Junbo Park  <https://orcid.org/0000-0001-8039-0317>

## REFERENCES

1. D. Y. Jung et al., *Power semiconductor SMD package embedded in multilayered ceramic for low switching loss*, ETRI J. **39** (2017), 866–873.
2. D. Y. Jung et al., *Multi-layer substrate based power semiconductor package for low parasitic inductance and high heat transfer*, in *Asia-Pacific Workshop Fundam. Applicat. Adv. Semicond. Devices (AWAD)*, Hakodate, Japan, July 2016, pp. 283–285.
3. A. Ball et al., *System design of 3D integrated non-isolated point of load converter*, in *Annu. IEEE Appl. Power Electron. Conf. Exposition*, Austin, TX, USA, Feb. 2008, pp. 181–186, doi: 10.1109/APEC.2008.4522719.
4. Q. Li et al., *High inductance density low-profile inductor structure for integrated point-of-load converter*, in *Annu. IEEE Appl. Power Electron. Conf. Exposition*, Washington, DC, USA, Feb. 2009, pp. 1011–1017, doi: 10.1109/APEC.2009.4802786.
5. Q. Li, Y. Dong, and F. C. Lee, *High-density low-profile coupled inductor design for integrated point-of-load converters*, IEEE Trans. Power Electron. **28** (2013), 547–554.
6. Y. Su et al., *Low profile LTCC inductor substrate for multi-MHz integrated POL converter*, in *Annu. IEEE Appl. Power Electron. Conf. Exposition (APEC)*, Orlando, FL, USA, Feb. 2012, pp. 1331–1337, doi: 10.1109/APEC.2012.6165992.
7. C. Nan, and R. Ayyanar, *A 1MHz bi-directional soft-switching DC-DC converter with planar coupled inductor for dual voltage automotive systems*, in *IEEE Appl. Power Electron. Conf. Exposition (APEC)*, Long Beach, CA, USA, Mar. 2016, pp. 432–439, doi: 10.1109/APEC.2016.7467908.
8. T. Kim and S. Kwak, *A flexible voltage bus converter for the 48-/12-V dual supply system in electrified vehicles*, IEEE Trans. Veh. Technol. **66** (2017), 2010–2018.
9. B. Li et al., *A high frequency high efficiency GaN based bi-directional 48V/12V converter with PCB coupled inductor for mild hybrid vehicle*, in *IEEE Workshop Wide Bandgap Power Devices Applicat.*, Atlanta, GA, USA, 2018, pp. 204–211, doi: 10.1109/WiPDA.2018.8569067.
10. M. H. Ahmed et al., *48-V voltage regulator module with PCB winding matrix transformer for future data centers*, IEEE Trans. Ind. Electron. **64** (2017), 9302–9310.
11. D. Reusch, S. Biswas, and Y. Zhang, *System optimization of a high power density non-isolated intermediate bus converter for 48 V server applications*, in *E Appl. Power Electron. Conf. Exposition*, San Antonio, TX, USA, Mar. 2018, pp. 2191–2197, doi: 10.1109/APEC.2018.8341320.
12. C. Fei et al., *Two-stage 48 V-12 V/6 V-1.8 V voltage regulator module with dynamic bus voltage control for light-load efficiency improvement*, IEEE Trans. Power Electron. **32** (2017), 5628–5636.
13. B. Hughes et al., *Increasing the switching frequency of GaN HFET converters*, in *IEEE Int. Electr. Devices Meeting (IEDM)*, Washington, DC, USA, Dec. 2015, pp. 16.7.1–16.7.4.
14. R. Mitova et al., *Current trends for GaN on Si power devices for industrial applications*, in *Int. Conf. Integr. Electron. Syst. (CIPS)*, Nuremberg, Germany, Mar. 2016, pp. 1–11.
15. W. Zhang et al., *A new package of high-voltage cascode gallium nitride device for megahertz operation*, IEEE Trans. Power Electron. **31** (2016), 1344–1353.
16. I. Omura et al., *Gallium nitride power HEMT for high switching frequency power electronics*, in *Int. Workshop Phys. Semicond. Devices*, Mumbai, India, Dec. 2007, pp. 781–786.
17. D. Y. Jung et al., *Design and evaluation of cascode GaN FET for switching power conversion systems*, ETRI J. **39** (2017), 62–68.
18. M. Kim et al., *Pulse-mode dynamic Ron measurement of large-scale high-power AlGaN/GaN HFET*, ETRI J. **39** (2017), 292–299.
19. W. Zhang et al., *High frequency high current point of load modules with integrated planar inductors*, in *IEEE Electron. Compon. Technol. Conf. (ECTC)*, Orlando, FL, USA, May 2014, pp. 504–511, doi: 10.1109/ECTC.2014.6897331.
20. D. Han, and B. Sarlioglu, *Deadtime effect on GaN-based synchronous boost converter and analytical model for optimal deadtime selection*, IEEE Trans. Power Electron. **31** (2016), 601–612.
21. J. Wang, Y. Li, and Y. Han, *Integrated modular motor drive design with GaN power FETs*, IEEE Trans. Ind. Applicat. **51** (2015), 3198–3207.

## AUTHOR BIOGRAPHIES



**Dong Yun Jung** received his BS degree in electronics and materials engineering (*First class honors*) from Kwangwoon University, Seoul, Rep. of Korea, in 2001, and his MS and PhD degrees (*excellence graduate*) in electrical engineering from the Korea Advanced Institute of Science and Technology (KAIST), Daejeon, Rep. of Korea, in 2003 and 2009, respectively. He studied broadband ICs for optical communications, and low-power CMOS receiver circuits and 3-D modules using low temperature co-fired ceramic (LTCC) technologies for millimeter-wave applications. He joined the Electronics and Telecommunications Research Institute (ETRI), Rep. of Korea in 2003 as an engineering researcher. From 2009 to 2014, he was with the R&D Center of Samsung Electronics, as a senior engineer, where he contributed to the development of millimeter-wave ICs. Since 2014, he has been with the ETRI as a principal researcher. His research interests include power electronics semiconductor devices and high-speed, high-efficiency power electronics conversions for high power and energy applications. Dr. Jung received the Best Paper Award from KAIST in 2007 and 2008, respectively. He received a Silver Award in the SAMSUNG Best Paper Award competition in 2012.



**Hyun Gyu Jang** received his BS degree in electronics engineering from the Korea Polytechnic University, Siheung, Rep. of Korea, in 2013, and his MS in advanced device technology from the University of Science, UST, Rep. of Korea, in 2015. He studied Gallium nitride power devices. In 2015, he joined the Electronics and Telecommunications Research Institute, located in Daejeon, Rep. of Korea, as a research engineer. His current research interests include the design, fabrication, and characterization of electronic devices based on compound semiconductors, and the design of power supply units, such as inverters and converters.



**Minki Kim** received his BS degree in electrical engineering and computer science from Kyungpook National University, Daegu, Rep. of Korea, in 2008 and his MS degree in electrical engineering and computer science from Seoul National University, Rep. of Korea, in 2010. Since 2010, he has been working at Electronics and Telecommunications Research Institute, Daejeon, Rep. of Korea as a research engineer. His research interests include wide band-gap power devices and power control systems.



**Junbo Park** received his BS degree in physics from Harvey Mudd College, Claremont, CA, USA in 2008. He received his PhD in applied physics from Cornell University Ithaca, NY, USA, in 2014. In 2015, he joined Electronics and Telecommunications Research Institute, Daejeon, Rep. of Korea I as a research scientist. His research interests include power electronics modules and power device fabrication. He is currently focused on SiC power devices.



**Chi-Hoon Jun** received his MS degree in mechanical engineering and his PhD degree in metallurgical engineering from Kyungpook National University, Daegu, Rep. of Korea, in 1984 and 1997, respectively. He joined the Electronics and Telecommunications Research Institute, Daejeon, Rep. of Korea in 1985 as a member of the engineering staff. He became a principal member in 1999. He also served as a team leader of the Microsystem team from 2001 to 2002. His primary research interests are in WBG power semiconductor devices, power packaging, energy harvesting, optical MEMS for telecommunication, physical microsensors, bioMEMS/biochips, surface micromachining, DRAM metallization, and CVD/MOCVD processes for advanced semiconductors. He received the Outstanding Researcher Award and the R&D Award from the Ministry of Science & Technology, Rep. of Korea, in 1987 and 1990, respectively.





**Jong Moon Park** received his BS and MS degrees in electronic engineering from Chonbuk National University, Jeonju, Rep. of Korea in 1982 and 1991, respectively. He received his PhD in semiconductor science technology from Chonbuk National University in 2010. Since 1985, he has been with Electronics and Telecommunications Research Institute (ETRI), Daejeon, Rep. of Korea, where he has been involved in semiconductor technology development of Si devices and lithography processes. He is currently the Director of the Convergence Component Technology Center of ETRI. His research interests include silicon detectors and Si/SiC power device fabrication.



**Sang Choon Ko** received his BS and MS degrees in electrical engineering from Sungkyunkwan University, Suwon, Rep. of Korea in 1994 and 1996, respectively. From 1990 to 1991, he served in the Korean army. After obtaining his MS degree, he transferred to Tohoku University, Sendai, Japan. He received his PhD from Tohoku University in March 1999. That year, he joined the Microsystem Technology Laboratory of DaimlerChrysler Co., Stuttgart, Germany, as a visiting researcher. At the same time, he was a research associate in the Department of Mechatronics and Electronics of Tohoku University. In 2000, he joined the Pohang University of Science and Technology, Rep. of Korea, in a postdoctoral position. Since October 2001, he has worked on the Microsystem Team of Electronics and Telecommunications Research Institute, Daejeon, Rep. of Korea. He has studied piezoelectric acoustic devices, condenser microphones, and MEMS optical switches. Since 2011, he has participated in the development of GaN-based discrete devices, e.g., SBDs and FETs.